Published in Organometallics 30, issue 5, pp. 942–951, 2011,
which should be used for any reference to this work

Template-Directed Synthesis of Hexanuclear Arene Ruthenium Complexes with Trigonal-Prismatic Architecture Based on 2,4,6-Tris(3-pyridyl)triazine Ligands

Julien Freudenreich, Julien Furrer, Georg Süss-Fink, and Bruno Therrien*

Institut de Chimie, Université de Neuchâtel, 51 Ave de Bellevaux, 2000 Neuchâtel, Switzerland

Cationic arene ruthenium metalla-prisms of the general formula $[Ru_6(p\text{-cymene})_6(3\text{-tpt})_2\text{-}(OO\cap OO)_3]^{6+}$ (3-tpt = 2,4,6-tris(3-pyridyl)-1,3,5-triazine; $OO\cap OO$ = 5,8-dioxido-1,4-naphthoqui-nonato $[\mathbf{1}]^{6+}$ or 6,11-dioxido-5,12-naphthacenedionato $[\mathbf{2}]^{6+}$) have been obtained from the corresponding dinuclear arene ruthenium complexes $[Ru_2(p\text{-cymene})_2(OO\cap OO)Cl_2]$ by reaction with 3-tpt, silver trifluoromethanesulfonate in the presence of an aromatic molecule (1,3,5-tribro-mobenzene, phenanthrene, pyrene, or triphenylene) that acts as a template. While the large template molecule triphenylene is permanently encapsulated in the metalla-prisms to give the complexes $[\text{triphenylene}\subset\mathbf{1}]^{6+}$ and $[\text{triphenylene}\subset\mathbf{2}]^{6+}$, 1,3,5-tribromobenzene can be removed in toluene, thus leaving the empty cages $[\mathbf{1}]^{6+}$ and $[\mathbf{2}]^{6+}$, which are isolated as their trifluoromethanesulfonate salts. In the case of the metalla-prism connected by the 5,8-dioxido-1,4-naphthoquinonato bridging ligands, the NMR spectrum reveals two isomers, **1a** and **1b**, the formation of which can be rationalized by means of multiple NMR experiments (one-dimensional, two-dimensional, ROESY, and DOSY). The empty and filled metalla-prisms, $[\mathbf{1}]^{6+}$, $[\mathbf{2}]^{6+}$, $[\text{template}\subset\mathbf{1}]^{6+}$, and $[\text{template}\subset\mathbf{2}]^{6+}$, have been characterized by NMR, UV−vis, and IR spectroscopy. The slow exchange processes of a guest molecule moving in and out of the cavity of cages $[\mathbf{1}]^{6+}$ and $[\mathbf{2}]^{6+}$ have been studied in solution with phenanthrene and pyrene. One-dimensional exchange spectroscopic (1D EXSY) measurements show that $[\text{phenanthrene}\subset\mathbf{1}]^{6+}$ is in a faster exchange regime than $[\text{phenanthrene}\subset\mathbf{2}]^{6+}$ and that phenanthrene is more easily exchanged than pyrene in cages $[\mathbf{1}]^{6+}$ and $[\mathbf{2}]^{6+}$, all observations being consistent with the portal size of the cages.

Introduction

Well-defined supramolecular metalla-assemblies using 2,4,6-tris(4-pyridyl)triazine (4-tpt) ligands are quite common: The extended and potentially planar tetra-aryl ring system with multiple coordinating groups at the periphery has been judiciously exploited to afford a wide variety of supramolecular assemblies with different metal centers.[1] On the other hand, metalla-assemblies incorporating the isomeric (3-pyridyl)triazine derivative, 2,4,6-tris(3-pyridyl)-triazine (3-tpt), are rare.

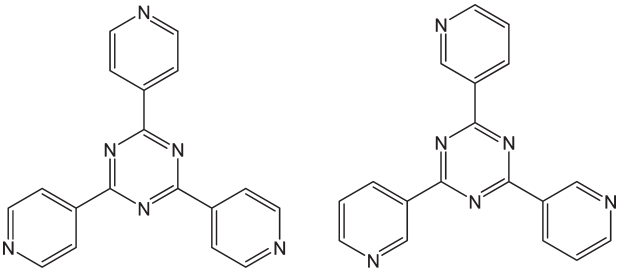

Bowl-shaped hexanuclear Pd or Pt coordination cages, $[M_6(en)_6(3\text{-tpt})_4]^{12+}$ (en = ethylenediamine), able to encapsulate guest molecules have been described by Fujita[2] (Figure 1A). The trinuclear rhenium tricarbonyl diimine

*To whom correspondence should be addressed. E-mail: bruno.therrien@unine.ch.

(1) (a) Fujita, M.; Oguro, D.; Miyazawa, M.; Oka, H.; Yamaguchi, K.; Ogura, K. *Nature* **1995**, *378*, 469–471. (b) Webb, S. J.; Sanders, J. K. M. *Inorg. Chem.* **2000**, *39*, 5912–5919. (c) Manimaran, B.; Rajendran, T.; Lu, Y.-L.; Lee, G.-H.; Peng, S.-M.; Lu, K.-L. *Eur. J. Inorg. Chem.* **2001**, 633–636. (d) Crowley, J. D.; Goshe, A. J.; Bosnich, B. *Chem. Commun.* **2003**, 2824–2825. (e) Kieran, A. L.; Bond, A. D.; Belenguer, A. M.; Sanders, J. K. M. *Chem. Commun.* **2003**, 2674–2675. (f) Sun, S.-S.; Anspach, J. A.; Lees, A. J. *Inorg. Chim. Acta* **2003**, *351*, 363–368. (g) Fujita, M.; Tominaga, M.; Hori, A.; Therrien, B. *Acc. Chem. Res.* **2005**, *38*, 369–378 and references cited therein. (h) Dinolfo, P. H.; Coropceanu, V.; Brédas, J.-L.; Hupp, J. T. *J. Am. Chem. Soc.* **2006**, *128*, 12592–12593. (i) Casanova, M.; Zangrando, E.; Munini, F.; Iengo, E.; Alessio, E. *Dalton Trans.* **2006**, 5033–5045. (j) Wu, J.-Y.; Chang, C.-H.; Thanasekaran, P.; Tsai, C.-C.; Tseng, T.-W.; Lee, G.-H.; Peng, S.-M.; Lu, K.-L. *Dalton Trans.* **2008**, 6110–6112. (k) Han, Y.-F.; Jia, W.-G.; Yu, W.-B.; Jin, G.-X. *Chem. Soc. Rev.* **2009**, *38*, 3419–3434 and references cited therein. (l) Therrien, B. *J. Organomet. Chem.* **2011**, *696*, 637–651.

(2) (a) Fujita, M.; Yu, S.-Y.; Kusukawa, T.; Funaki, H.; Ogura, K.; Yamaguchi, K. *Angew. Chem., Int. Ed.* **1998**, *37*, 2082–2085. (b) Yu, S.-Y.; Kusukawa, T.; Biradha, K.; Fujita, M. *J. Am. Chem. Soc.* **2000**, *122*, 2665–2666. (c) Yoshizawa, M.; Takeyama, Y.; Kusukawa, T.; Fujita, M. *Angew. Chem., Int. Ed.* **2002**, *41*, 1347–1349. (d) Kubota, Y.; Sakamoto, S.; Yamaguchi, K.; Fujita, M. *Proc. Natl. Acad. Sci. U.S.A.* **2002**, *99*, 4854–4856. (e) Yoshizawa, M.; Tamura, M.; Fujita, M. *Science* **2006**, *312*, 251–254.

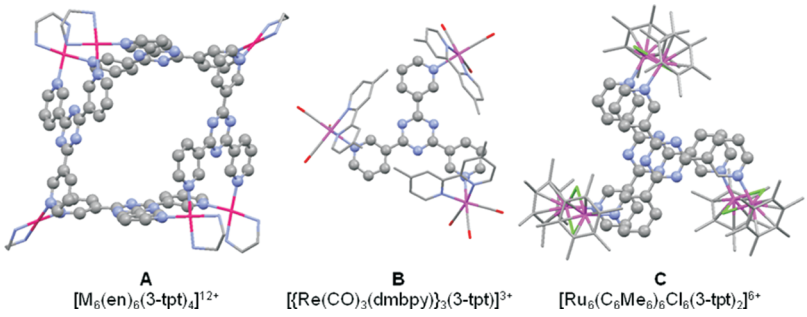

Figure 1. Discrete metalla-assemblies incorporating the 3-tpt ligand.[2−4].

complex, $[\{Re(CO)_3(dmbpy)\}_3(3\text{-tpt})]^{3+}$ (dmbpy = 4,4′-dimethyl-2,2′-bipyridine), which has a π-acidic cavity, showed good sensing affinity for F^- anions (Figure 1B).[3] Recently, we prepared hexanuclear arene ruthenium prisms, $[Ru_6(arene)_6Cl_6(3\text{-tpt})_2]^{6+}$ (arene = *p*-cymene or hexamethylbenzene), in which the two arene ruthenium 3-tpt panels were linked together in a face-to-face arrangement by chloro bridges.[4] Interestingly, two isomers were found for the *p*-cymene derivative, while only the 3-fold symmetric isomer was obtained for the hexamethylbenzene analogue (Figure 1C).

The difficulty of forming discrete metalla-assemblies with 3-tpt ligands resides in controlling the orientation of the pyridyl groups prior to coordination to the metal centers. As opposed to the 4-tpt isomer, in 3-tpt a rotation by 180° of one of the three C−C triazine−pyridyl bonds reduces the 3-fold symmetry, thus generating atropoisomerism before coordination. As a consequence, the synthesis and characterization of well-defined metalla-assemblies containing the tridentate 3-tpt ligand is difficult and hazardous.

In recent years, we have reported various hexacationic metalla-prisms incorporating the 4-tpt ligands.[5] The ability of these metalla-prisms to permanently encapsulate or to temporarily host aromatic molecules, according to the portal size of the cages, has been demonstrated.[6] However, all attempts to synthesize the equivalent metalla-prisms with 3-tpt instead of 4-tpt using the same synthetic strategy have failed, giving rise to only insoluble materials. We now found that the presence of an appropriate aromatic molecule, which acts as a template during the synthesis of the metalla-prisms, gives in excellent yield the cationic metalla-prismatic cations containing the template molecule, $[template\subset Ru_6(p\text{-cymene})_6(3\text{-tpt})_2(OO\cap OO)_3]^{6+}$ (*OO*∩*OO* = 5,8-dioxido-1,4-naphthoquinonato; $[template\subset\mathbf{1}]^{6+}$ or 6,11-dioxido-5,12-naphthacenedionato; $[template\subset\mathbf{2}]^{6+}$). Moreover, we observed that after formation of the metalla-prismatic cations, small template molecules can be removed, thus allowing us to study the host−guest properties of empty cages $[\mathbf{1}]^{6+}$ and $[\mathbf{2}]^{6+}$ in solution.

Results and Discussion

The template-containing hexanuclear arene ruthenium cations $[template\subset\mathbf{1}]^{6+}$ and $[template\subset\mathbf{2}]^{6+}$ are prepared in a two-step strategy, in which the known dinuclear 5,8-dioxido-1,4-naphthoquinonato (dhnq) complex[6d] $[Ru_2(p\text{-cymene})_2(dhnq)Cl_2]$ or the 6,11-dioxido-5,12-naphthacenedionato (dhtq) complex[7] $[Ru_2(p\text{-cymene})_2(dhtq)Cl_2]$ is used as a bimetallic connector, followed by addition of an aromatic template (1,3,5-tribromobenzene, phenanthrene, pyrene, or triphenylene) and 3-tpt (see Scheme 1). All cationic complexes are isolated as their trifluoromethanesulfonate salts in good yield.

Interestingly, the composition of the products depends on the nature of the clip and of the template used during the assembly of the organometallic cage. In the case of the bimetallic clip $[Ru_2(p\text{-cymene})_2(dhnq)]^{2+}$ and the smaller templates 1,3,5-tribromobenzene, phenanthrene, and pyrene, a mixture comprising two sets of signals is observed in the ^{1}H NMR spectrum, $[template\subset\mathbf{1a}]^{6+}$ and $[template\subset\mathbf{1b}]^{6+}$. In both systems, the aromatic template is shown to be encapsulated. However, with triphenylene, only one highly symmetrical structure is observed, $[triphenylene\subset\mathbf{1a}]^{6+}$. These observations suggest the existence of two isomers of **1**, as depicted in Figure 2, in accordance with the analogous chloro-bridged hexanuclear arene ruthenium prism $[Ru_6(p\text{-cymene})_6Cl_6(3\text{-tpt})_2]^{6+}$.[4] Isomer **1a** shows equivalent pyridyl and *p*-cymene protons, while isomer **1b** contains three nonequivalent pyridyl and *p*-cymene groups. The presence of these two isomers was further confirmed by a range of NMR experiments [one-dimensional (1D), two-dimensional, COSY, and ROESY].

In the case of the larger bimetallic clip $[Ru_2(p\text{-cymene})_2(dhtq)]^{2+}$, only one set of signals is observed with all the templates, suggesting the presence of the highly symmetrical isomer. However, with 1,3,5-tribromobenzene, phenanthrene, and pyrene, the encapsulation of the template is not quantitative, the empty metalla-prism $[\mathbf{2}]^{6+}$ being observed as well by NMR spectroscopy. The relative quantity of the empty prism is dependent on the size of the template: the smaller the template, the greater the quantity of the empty prism. With triphenylene, only the template-containing cage is observed. Obviously, triphenylene fits perfectly in the

(3) Hung, C.-Y.; Singh, A. S.; Chen, C.-W.; Wen, Y.-S.; Sun, S.-S. *Chem. Commun.* **2009**, 1511–1513.
(4) Govindaswamy, P.; Süss-Fink, G.; Therrien, B. *Organometallics* **2007**, *26*, 915–924.
(5) (a) Govindaswamy, P.; Linder, D.; Lacour, J.; Süss-Fink, G.; Therrien, B. *Chem. Commun.* **2006**, 4691–4693. (b) Govindaswamy, P.; Linder, D.; Lacour, J.; Süss-Fink, G.; Therrien, B. *Dalton Trans.* **2007**, 4457–4463. (c) Therrien, B. *Eur. J. Inorg. Chem.* **2009**, 2445–2453.
(6) (a) Therrien, B.; Süss-Fink, G.; Govindaswamy, P.; Renfrew, A. K.; Dyson, P. J. *Angew. Chem., Int. Ed.* **2008**, *47*, 3773–3776. (b) Mattsson, J.; Govindaswamy, P.; Furrer, J.; Sei, Y.; Yamaguchi, K.; Süss-Fink, G.; Therrien, B. *Organometallics* **2008**, *27*, 4346–4356. (c) Govindaswamy, P.; Furrer, J.; Süss-Fink, G.; Therrien, B. *Z. Anorg. Allg. Chem.* **2008**, *634*, 1349–1352. (d) Barry, N. P. E.; Therrien, B. *Eur. J. Inorg. Chem.* **2009**, 4695–4700. (e) Zava, O.; Mattsson, J.; Therrien, B.; Dyson, P. J. *Chem.—Eur. J.* **2010**, *16*, 1428–1431. (f) Freudenreich, J.; Barry, N. P. E.; Süss-Fink, G.; Therrien, B. *Eur. J. Inorg. Chem.* **2010**, 2400–2405. (g) Mattsson, J.; Zava, O.; Renfrew, A. K.; Sei, Y.; Yamaguchi, K.; Dyson, P. J.; Therrien, B. *Dalton Trans.* **2010**, *39*, 8248–8255.
(7) Barry, N. P. E.; Furrer, J.; Therrien, B. *Helv. Chim. Acta* **2010**, *93*, 1313–1328.

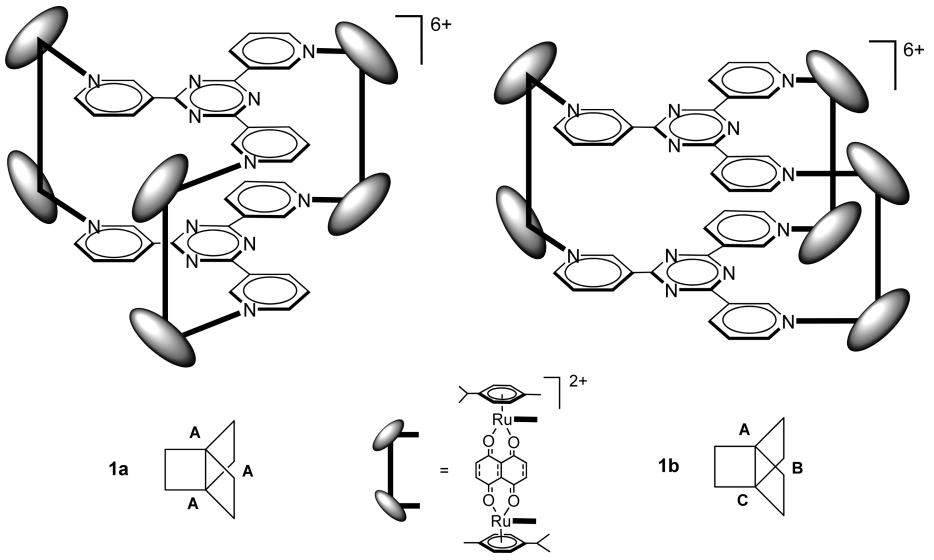

Figure 2. Schematic representations of symmetrical isomer **1a** (left) and unsymmetrical isomer **1b** (right) with the identification of their respective trigonal segments.

Scheme 1. Template-Directed Synthesis of Metalla-Prisms $[1]^{6+}$ and $[2]^{6+}$

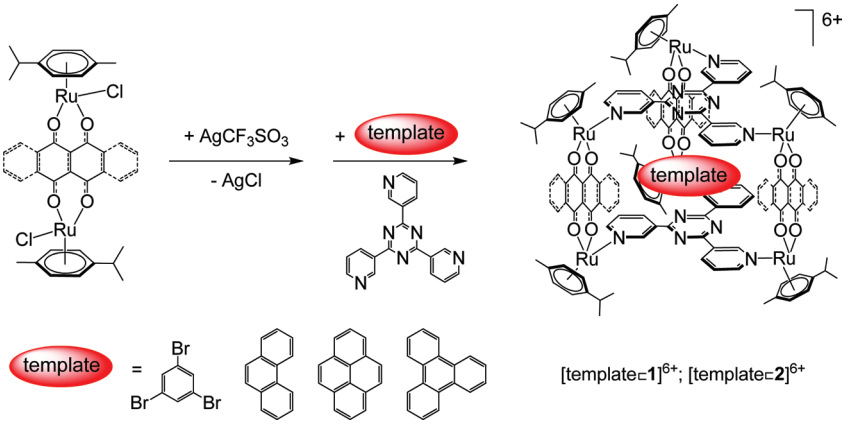

cavity of **1** and **2**, thus generating exclusively the symmetrical isomer [triphenylene⊂**1a**]$^{6+}$ and [triphenylene⊂**2**]$^{6+}$, in which all segments of the triangular prism are equivalent. The ^{1}H NMR spectra of the two highly symmetrical systems encapsulating triphenylene are presented in Figure 3. It is worth noting that an unsymmetrical isomer for **2** is not observed, because of the width of the dhtq bridging ligand that does not allow two bimetallic clips to share the same segment.

The formation of metalla-assemblies $[1]^{6+}$ and $[2]^{6+}$ was also confirmed by electrospray mass spectrometry, the two cage molecules displaying good stability. The ESI-MS spectra show peaks corresponding to $[1 + (CF_3SO_3)_4]^{2+}$ and $[2 + (CF_3SO_3)_4]^{2+}$ at m/z 1599.61 and 1749.20, respectively (Figure S1 of the Supporting Information). Moreover, for the most stable system, the guest molecule is retained inside the cavity under electrospray conditions, thus giving a peak at m/z 1863.17 corresponding to [**2** + triphenylene + $(CF_3SO_3)_4]^{2+}$ (Figure S2 of the Supporting Information). These peaks are unambiguously assigned on the basis of their characteristic Ru_6 isotope patterns.

The encapsulation of template molecules in $[1]^{6+}$ and $[2]^{6+}$ was further confirmed by diffusion-ordered NMR spectroscopy (DOSY).[8] The DOSY spectra of all [template⊂**cage**]$^{6+}$ systems show the same diffusion coefficient for the host and the guest, thus proving the encapsulation of the aromatic template in the cavity of $[1]^{6+}$ and $[2]^{6+}$. As an example, the DOSY spectra of [phenanthrene⊂**2**]$^{6+}$ are presented in Figure 4. This figure clearly shows the encapsulation of phenanthrene in the cavity of $[2]^{6+}$ not only from the upfield shift and splitting of the signals but from the diffusion coefficient of the [phenanthrene⊂**2**]$^{6+}$ system that is equivalent to the diffusion coefficient of the empty cage (6.3×10^{-10} m^2 s^{-1}, CD_3CN, 25 °C).

Electronic absorption spectra of [template⊂**1**]$^{6+}$ and [template⊂**2**]$^{6+}$ have been measured in dichloromethane at a concentration of 10^{-5} M in the range of 200−800 nm (Figures 5 and 6, respectively). The UV−visible spectra of all complexes are characterized by an intense high-energy band centered at 280 nm, which is assigned to a ligand-localized or intraligand $\pi \rightarrow \pi^*$ transition, and a series of broad low-energy bands associated to metal-to-ligand

(8) (a) Wu, D. H.; Chen, A.; Johnson, C. S., Jr. *J. Magn. Reson., Ser. A* **1995**, *115*, 123–126. (b) Johnson, C. S., Jr. *Prog. Nucl. Magn. Reson. Spectrosc.* **1999**, *34*, 203–256. (c) Ajami, D.; Rebek, J., Jr. *Angew. Chem., Int. Ed.* **2007**, *46*, 9283–9286. (d) Lemonnier, J.-F.; Floquet, S.; Kachmar, A.; Rohmer, M.-M.; Bénard, M.; Marrot, J.; Terazzi, E.; Piguet, C.; Cadot, E. *Dalton Trans.* **2007**, 3043–3054.

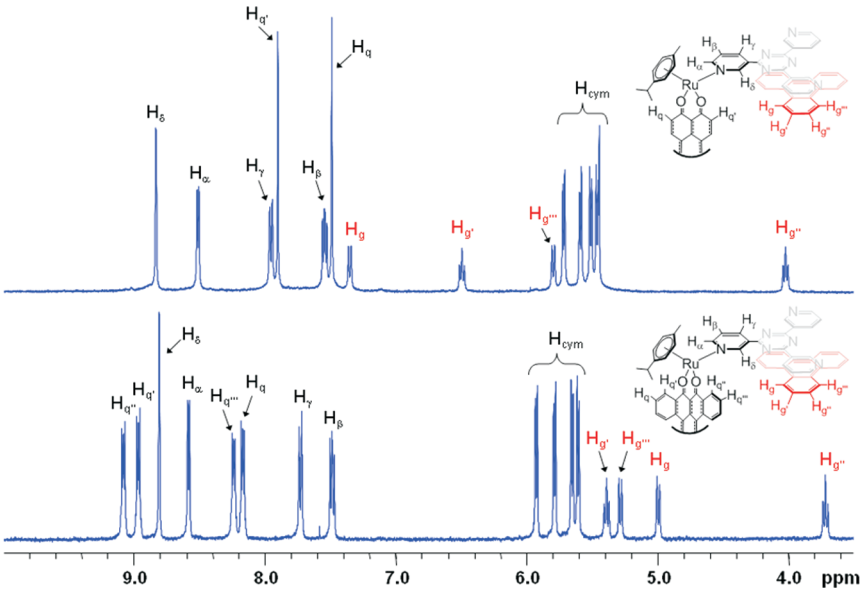

Figure 3. ^{1}H NMR spectra of [triphenylene⊂**1a**]$^{6+}$ (top) and [triphenylene⊂**2**]$^{6+}$ (bottom).

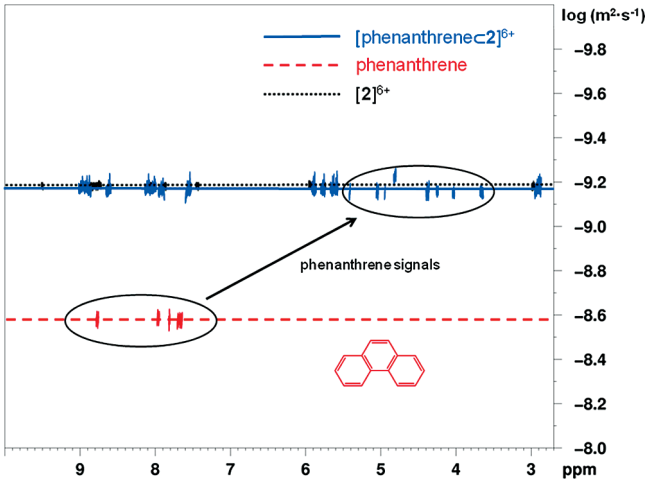

Figure 4. DOSY NMR spectra of phenanthrene, [**2**]$^{6+}$, and [phenanthrene⊂**2**]$^{6+}$ in CD_3CN at 25 °C.

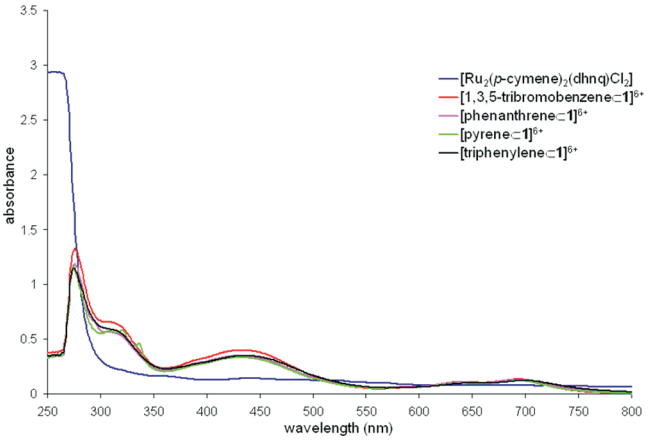

Figure 5. UV−visible spectra of [Ru_2(*p*-cymene)(dhnq)Cl_2] and [template⊂**1**]$^{6+}$ in dichloromethane at 10^{-5} M.

charge transfer (MLCT) transitions. In the [template⊂**1**]$^{6+}$ series, in which the dhnq ligands are used, the MLCT bands are found at ≈430, 640, and 695 nm, while in the [template⊂**2**]$^{6+}$ series incorporating dhtq ligands, these three MLCT bands are significantly blue-shifted and are found at 375, 565, and 610 nm, respectively. A similar blue shift is observed between the MLCT bands of the dinuclear complexes [Ru_2(*p*-cymene)$_2$(dhnq)Cl_2] and [Ru_2-(*p*-cymene)$_2$(dhtq)Cl_2],[7] but there might also be a contribution from intraligand charge transfer (ILCT) transitions of the ligands.

The template in the [1,3,5-tribromobenzene⊂**cage**]$^{6+}$ host−guest systems can be removed in refluxing toluene, thus giving rise to empty metalla-cages [**1**]$^{6+}$ and [**2**]$^{6+}$ that can be isolated as the trifluoromethanesulfonate salts. Metalla-cage [**1**]$^{6+}$ is obtained as a mixture of isomers [**1a**]$^{6+}$ and [**1b**]$^{6+}$, while for [1,3,5-tribromobenzene⊂**2**]$^{6+}$, only salt [**2**][CF_3SO_3]$_6$ is isolated after workup. The host−guest properties of these empty metalla-cages have been studied in solution using various NMR techniques. Upon gradual

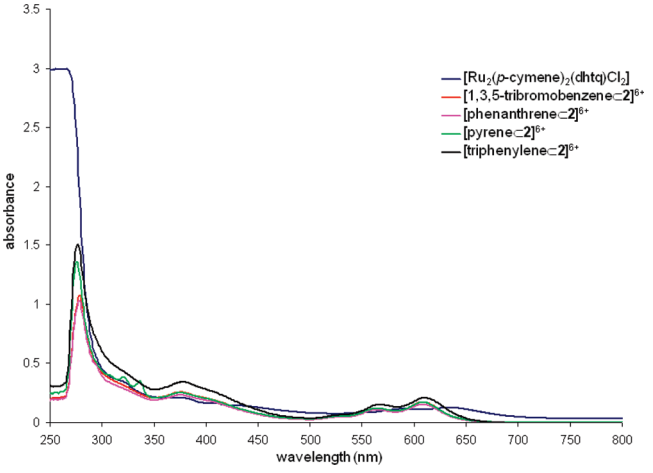

Figure 6. UV−visible spectra of [Ru_2(*p*-cymene)(dhtq)Cl_2] and [template⊂**2**]$^{6+}$ in dichloromethane at 10^{-5} M.

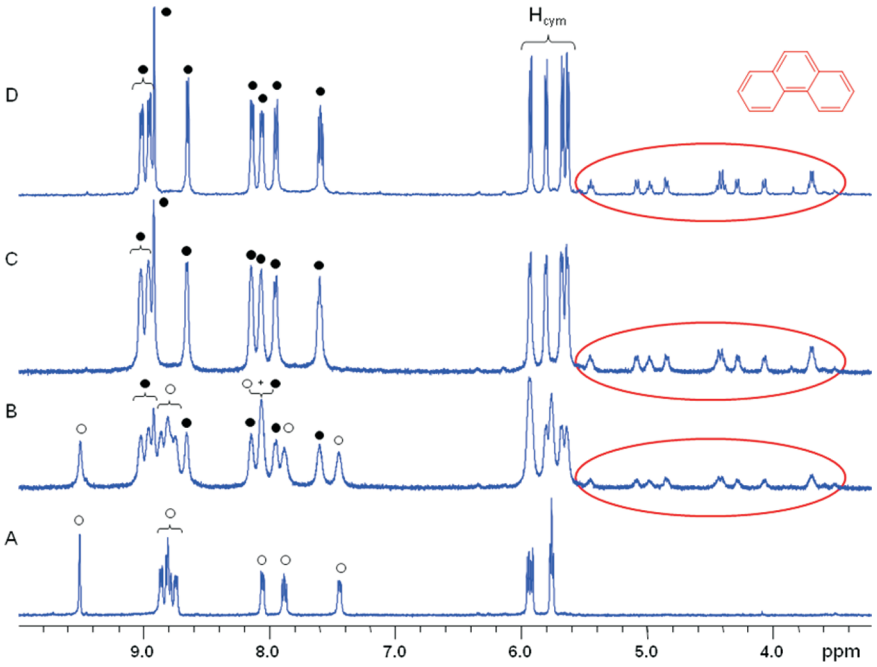

Figure 7. ^{1}H NMR titration of phenanthrene in a CD_3CN solution of $[\mathbf{2}]^{6+}$ (25 °C) with 0.0 equiv (A), 0.5 equiv (B), 1.0 equiv (C), and the [phenanthrene⊂$\mathbf{2}$]$^{6+}$ complex (D) showing the empty cage signals (○) and filled cage signals (●).

addition of phenanthrene to $[\mathbf{2}]^{6+}$ (CD_3CN, 25 °C), a new set of signals corresponding to [phenanthrene⊂$\mathbf{2}$]$^{6+}$ emerges, and no chemical shift of the host or of the guest signals is observed (Figure 7). This suggests a rapid encapsulation of the guest and a slow exchange process.

Interestingly, upon gradual addition of triphenylene to a stoichiometric mixture of $[\mathbf{1a}]^{6+}$ and $[\mathbf{1b}]^{6+}$ (CD_3CN, 25 °C), encapsulation of triphenylene occurs. Only the signals of cage $[\mathbf{1a}]^{6+}$ are affected by the addition of triphenylene up to 0.5 equiv of triphenylene added, which corresponds to the complete formation of [triphenylene⊂$\mathbf{1a}$]$^{6+}$ (see Figure S20 of the Supporting Information). The ^{1}H signals of cage $[\mathbf{1b}]^{6+}$ start to respond to the presence of triphenylene only if more than 0.5 equiv of triphenylene is present. The encapsulation process is fast on the NMR time scale, but the exchange tends toward zero. This has been verified using 1D EXSY experiments, in which no cross-peak is observed after selective inversion of the H_δ resonance, even with a 2 s mixing time (Figure S24 of the Supporting Information). Therefore, during the NMR measurements, the disappearance of the signals of cage $[\mathbf{1a}]^{6+}$ is accompanied by the emergence of the signals corresponding to [triphenylene⊂$\mathbf{1a}$]$^{6+}$, and then the signals of empty cage $[\mathbf{1b}]^{6+}$ disappeared slowly to give rise to a new set of signals corresponding to [triphenylene⊂$\mathbf{1b}$]$^{6+}$. Surprisingly, no competition for triphenylene is observed between cages $[\mathbf{1a}]^{6+}$ and $[\mathbf{1b}]^{6+}$, suggesting a strong preference of triphenylene for the cavity of $[\mathbf{1a}]^{6+}$, despite the presence of a large portal in $[\mathbf{1b}]^{6+}$ (segment C, Figure 2). In addition, the exchange between triphenylene and $[\mathbf{1b}]^{6+}$ also tends toward zero at −30 °C. This has been verified with a 1D EXSY experiment recorded with a 1 s mixing time, in which no cross-peak is observed after selective inversion of the H_δ resonance (Figure S25 of the Supporting Information). Moreover, DOSY spectra after addition of a second equivalent of triphenylene show all signals of [triphenylene⊂$\mathbf{1a}$]$^{6+}$ and [triphenylene⊂$\mathbf{1b}$]$^{6+}$ to diffuse at the same rate, while

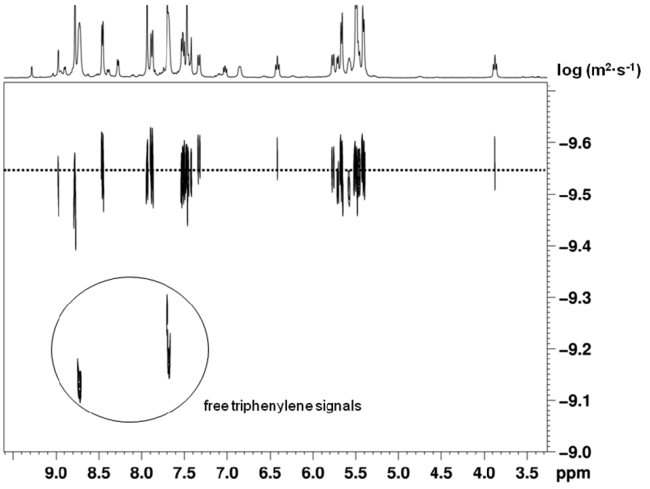

Figure 8. DOSY NMR spectra of 2 equiv of triphenylene in the presence of 1 equiv of cage $[\mathbf{1}]^{6+}$ (CD_3CN, −30 °C).

the excess of triphenylene that is not encapsulated diffuses more rapidly (see Figure 8).

The strong affinity of $[\mathbf{1a}]^{6+}$ for triphenylene as compared to that of cage $[\mathbf{1b}]^{6+}$ is further confirmed by a competition experiment in which 0.5 equiv of pyrene is first introduced into a mixture of $[\mathbf{1a}]^{6+}$ and $[\mathbf{1b}]^{6+}$ (CD_3CN, 25 °C). Then, 0.5 equiv of triphenylene is added, and the ^{1}H NMR spectrum is recorded. Once again, [triphenylene⊂$\mathbf{1a}$]$^{6+}$ is exclusively observed, the pyrene molecule being either in the cavity of $[\mathbf{1b}]^{6+}$ or in solution and the signals of $[\mathbf{1b}]^{6+}$ being broad (Figure S20 of the Supporting Information).

Variable-temperature measurements have also been performed (Figure S21 of the Supporting Information). In these spectra, it can be seen that the ^{1}H resonances of [triphenylene⊂$\mathbf{1b}$]$^{6+}$ are shifted and broadened already at −10 °C, indicating that there is an exchange between

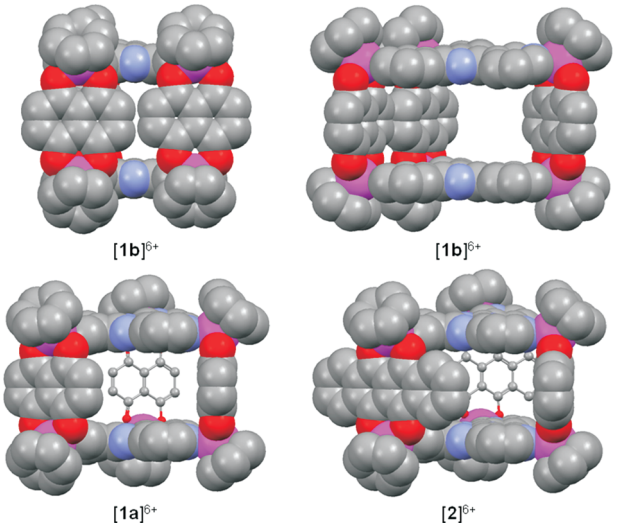

Figure 9. Chem3D simulations of metalla-prisms $[\mathbf{1a}]^{6+}$, $[\mathbf{1b}]^{6+}$, and $[\mathbf{2}]^{6+}$.

encapsulated triphenylene and free triphenylene. At 25 °C (Figure S21D of the Supporting Information), the ^{1}H signals of $[\mathbf{1b}]^{6+}$ become very broad and are almost invisible. By contrast, the ^{1}H resonances of $[\mathbf{1a}]^{6+}$ remain almost at the same chemical shifts and do not show an additional broadening at 70 °C. Likewise, the 12 weak resonances corresponding to triphenylene encapsulated in $[\mathbf{1b}]^{6+}$ become broad at −10 °C and are not detected starting from a temperature of 10 °C. However, as the temperature is increased, the resonances corresponding to triphenylene encapsulated in $[\mathbf{1a}]^{6+}$ remain sharp and do not show the typical downfield shift indicating an exchange process between encapsulated triphenylene and free triphenylene.

The reason for this high selectivity of cage $[\mathbf{1a}]^{6+}$ over cage $[\mathbf{1b}]^{6+}$ for the encapsulation of triphenylene in CD_3CN is not clear; however, the presence of three different portal sizes in $[\mathbf{1b}]^{6+}$ is certainly not an advantage as the smallest portal in which two bimetallic clips are facing each other reduces significantly the adaptability of the overall structure to accommodate the guest molecule. Molecular models of metalla-prisms $[\mathbf{1a}]^{6+}$, $[\mathbf{1b}]^{6+}$, and $[\mathbf{2}]^{6+}$ generated by Chem3D to estimate the portal size of these cages are presented in Figure 9. In addition, the symmetry of the cage and of the guest is a perfect match for [triphenylene⊂$\mathbf{1a}$]$^{6+}$, while for [triphenylene⊂$\mathbf{1b}$]$^{6+}$, an unsymmetrical system is obtained, in which 12 independent signals are observed for the encapsulated triphenylene molecule. Therefore, to gain further insight into this particular behavior of cages $[\mathbf{1a}]^{6+}$ and $[\mathbf{1b}]^{6+}$, the host−guest properties in solution of these systems along with cage $[\mathbf{2}]^{6+}$ were studied by NMR spectroscopy.

In this respect, two-dimensional EXSY ^{1}H NMR spectroscopy[9] proved to be useful[10] for those kind of systems in which exchange is slow on the NMR time scale. For our systems (Scheme 2), however, 1D selective EXSY experiments[11] appear to be more attractive, because the amount of sample available is fairly limited and the aromatic regions in the ^{1}H spectra are rather crowded. Guest binding induces shifts in several NMR signals from the host and all of those from the guest. Depending on the cages, we chose the H_δ protons of tpt to measure association constants, because they underwent large shifts under encapsulation and are well-removed from other signals (see Figure 3).

Figure 10 shows an example of a 1D EXSY spectrum recorded with [phenanthrene⊂$\mathbf{1a}$]$^{6+}$ in CD_3CN and the plot of the diagonal (inverted peak) and cross-peak (EXSY response) intensity as a function of the mixing time (τ_m). In our case, diagonal peaks represent the empty cage, whereas the cross-peak represents the cage in which the guest is encapsulated, or vice versa, depending on how well the signals are removed from other signals. Diagonal peaks, which have a relative amplitude of $0.5(1 + e^{-2k\tau_m})e^{-\tau_m/T_1}$, represent the nonexchanged magnetization,[12] whereas the cross-peaks, with a relative intensity of $0.5(1 - e^{-2k\tau_m})e^{-\tau_m/T_1}$, represent the exchanging magnetization from the encapsulation process. From these curves, the exchange rate k can be roughly determined. For instance, the curves of the H_δ protons of tpt in [phenanthrene⊂$\mathbf{1a}$]$^{6+}$ can be fitted with an exchange rate of ~3 s^{-1} at −30 °C.

The exchange rates (k) found for [guest⊂$\mathbf{1a}$]$^{6+}$ and [guest⊂$\mathbf{2}$]$^{6+}$ host−guest systems are summarized in Table 1. The results corroborate the observations and conclusions made for the encapsulation of triphenylene in $[\mathbf{1}]^{6+}$ and $[\mathbf{2}]^{6+}$. It clearly appears that the portal size strongly influences the adaptability of the overall structure to accommodate the different guests. For instance, [pyrene⊂$\mathbf{2}$]$^{6+}$ is in the slow exchange regime at 25 °C (k = 0.1 s^{-1}), showing that pyrene cannot easily leave $[\mathbf{2}]^{6+}$, because the adaptability of the overall structure to accommodate pyrene is high. As expected, the exchange of pyrene can be moderately accelerated when the measurements are taken at 45 °C (k = 0.8 s^{-1}). On the other hand, [pyrene⊂$\mathbf{1}$]$^{6+}$ comes into the slow exchange regime only at −30 °C (k = 0.2 s^{-1}). The exchange of pyrene can be significantly accelerated when the measurements are taken at −10 °C (k = 2.8 s^{-1}). This shows that pyrene can easily leave $[\mathbf{1}]^{6+}$, because the larger portal size of $[\mathbf{1}]^{6+}$ as compared to the portal size of $[\mathbf{2}]^{6+}$ decreases the adaptability of $[\mathbf{1}]^{6+}$ to accommodate pyrene. At 25 °C, the exchange process of [pyrene⊂$\mathbf{1}$]$^{6+}$ is in the intermediate regime, close to the coalescence temperature, because the ^{1}H spectrum displays broadened resonances and most of the resonances corresponding to the free pyrene and to the encapsulated pyrene as well as to the empty cage and to the cage with pyrene encapsulated merge into one broad "at-topped" resonance.

Likewise, [phenanthrene⊂$\mathbf{2}$]$^{6+}$ is in a moderate exchange regime at 25 °C (k = 3.0 s^{-1}), showing that phenanthrene can relatively easily leave $[\mathbf{2}]^{6+}$, because the adaptability of the overall structure to accommodate phenanthrene is lower than with pyrene. Similarly, [phenanthrene⊂$\mathbf{1a}$]$^{6+}$ is already in a moderate exchange regime at −30 °C (k = 2.6 s^{-1}), indicating that phenanthrene can very easily leave $[\mathbf{1a}]^{6+}$, because the adaptability of the overall structure to accommodate phenanthrene is correspondingly lower than with pyrene. As expected, at 25 °C, the exchange process of [phenanthrene⊂$\mathbf{1a}$]$^{6+}$ is in the fast regime, because the ^{1}H spectrum displays fairly sharp resonances and most of the resonances corresponding to the free phenanthrene and to

(9) Jeener, J.; Meier, B. H.; Bachmann, P.; Ernst, R. R. *J. Chem. Phys.* **1979**, *71*, 4546–4553.
(10) (a) Laughrey, Z. R.; Gibb, C. L. D.; Senechal, T.; Gibb, B. C. *Chem.—Eur. J.* **2003**, *9*, 130–139. (b) Szumna, A. *Chem. Commun.* **2009**, *2009*, 4191–4193.
(11) Stott, K.; Keeler, J.; Van, Q. N.; Shaka, A. J. *J. Magn. Reson.* **1997**, *125*, 302–324.
(12) McConnell, H. M. *J. Chem. Phys.* **1958**, *28*, 430–431.

Scheme 2. Exchange Processes

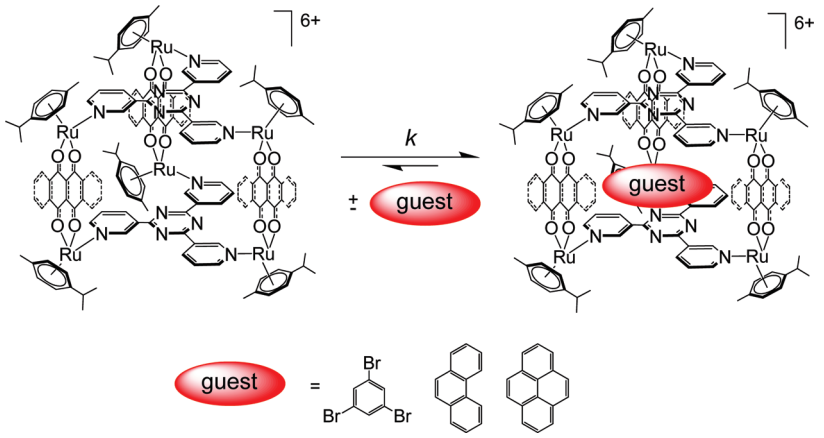

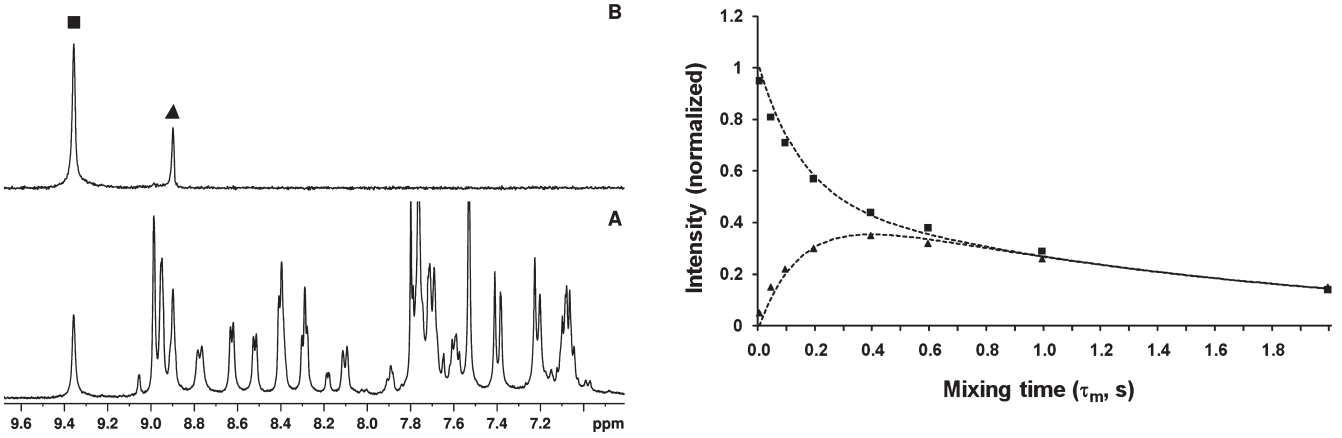

Figure 10. Excerpts of the aromatic part of the 1D ^{1}H NMR spectrum of (A) [phenanthrene⊂**1a**]$^{6+}$ and of the corresponding 1D selective EXSY spectrum recorded with a mixing time (τ_m) of 100 ms after selective excitation of the H_δ protons of tpt (B) at 9.35 ppm and plots of the diagonal (■) and cross-peak (▲) as a function of mixing time (τ_m). The spectra were recorded after addition of 0.5 equiv of phenanthrene. The diagonal peak corresponds to the empty cage, whereas the cross-peak corresponds to the cage with phenanthrene encapsulated. The dashed lines represent the best fit obtained by varying k in the McConnell equations,[12] $0.5(1 + e^{-2k\tau_m})e^{-\tau_m/T_1}$ for diagonal peaks and $0.5(1 - e^{-2k\tau_m})e^{-\tau_m/T_1}$ for cross-peaks. The T_1 relaxation times of the diagonal and the cross-peaks have been obtained using a classical inversion recovery experiment and have been incorporated into the equations described above for the fit.

Table 1. Calculated Equilibrium Constants (exchange rates) k between the Various Hosts and Guests Presented in This Work[a]

host	guest	temp (°C)	k (s^{-1})
[**1a**]$^{6+}$	phenanthrene	−30	2.6
[**2**]$^{6+}$	phenanthrene	25	3.0
[**1a**]$^{6+}$	pyrene	−30	0.2
[**1a**]$^{6+}$	pyrene	−10	2.8
[**2**]$^{6+}$	pyrene	25	0.1
[**2**]$^{6+}$	pyrene	45	0.8

[a] The k values have been calculated after addition of 0.5 equiv of guest to the host, and using the McConnell equations.[12]

the encapsulated phenanthrene as well as to the empty cage and to the cage with phenanthrene encapsulated merge into one sharp resonance.

To identify the existence of [phenanthrene⊂**1b**]$^{6+}$ and [pyrene⊂**1b**]$^{6+}$, a solution of [**1**]$^{6+}$ after addition of 0.75 equiv of phenanthrene and a solution of [**1**]$^{6+}$ after addition of 0.75 equiv of pyrene were prepared and their ^{1}H spectra recorded at −30 °C. If the lifetime of [phenanthrene⊂**1b**]$^{6+}$ and [pyrene⊂**1b**]$^{6+}$ was sufficiently long to be detected, both the resonances of [**1b**]$^{6+}$ and [phenanthrene⊂**1b**]$^{6+}$ and the resonances of [**1b**]$^{6+}$ and [pyrene⊂**1b**]$^{6+}$, respectively, should be observable. In those spectra, however, neither resonances indicating the presence of encapsulated phenanthrene or pyrene in [**1b**]$^{6+}$ nor resonances indicating the presence of [phenanthrene⊂**1b**]$^{6+}$ and [pyrene⊂**1b**]$^{6+}$ could be found (Figure S29 of the Supporting Information). This corroborates the results for triphenylene, namely a strong preference of phenanthrene and pyrene for the cavity of [**1a**]$^{6+}$. Because phenanthrene and pyrene are smaller than triphenylene, the portal sizes and the geometry of [**1b**]$^{6+}$ do not allow smaller molecules like phenanthrene or pyrene to remain on the NMR time scale in the cavity of [**1b**]$^{6+}$ for a sufficient amount of time.

In conclusion, a series of cationic arene ruthenium metalla-prisms built in the presence of a template from 3-tpt and dinuclear arene ruthenium complexes have been prepared and characterized. The empty cages were isolated by removal of the small template 1,3,5-tribromobenzene, thus allowing the host−guest properties of the complexes to be studied in solution. The estimated equilibrium constants obtained for the different host−guest systems were all consistent with the portal size and structure of the arene ruthenium metalla-prisms.

Experimental Section

General. $[Ru_2(p\text{-cymene})_2(dhnq)Cl_2]$,[6d] $[Ru_2(p\text{-cymene})_2(dhtq)Cl_2]$,[7] and 2,4,6-tris(3-pyridyl)-1,3,5-triazine[13] (3-tpt) were prepared according to published methods, and all other reagents were commercially available (Sigma-Aldrich, TCI Europe) and used as received. The ^1H, $^{13}C\{^1H\}$, ^1H DOSY, and ^1H ROESY NMR spectra were recorded on a Bruker AvanceII 400 spectrometer by using the residual protonated solvent as an internal standard. Infrared spectra were recorded as KBr pellets on a Perkin-Elmer FTIR 1720 X spectrometer. Elemental analyses were performed by the Mikroelementarisches Laboratorium, ETH Zürich (Zürich, Switzerland). Electrospray ionization mass spectra were recorded in positive-ion mode with a Bruker FTMS 4.7T BioAPEX II mass spectrometer (University of Fribourg, Fribourg, Switzerland). UV−visible absorption spectra were recorded with a Uvikon 930 spectrometer by using precision cells made of quartz (1 cm).

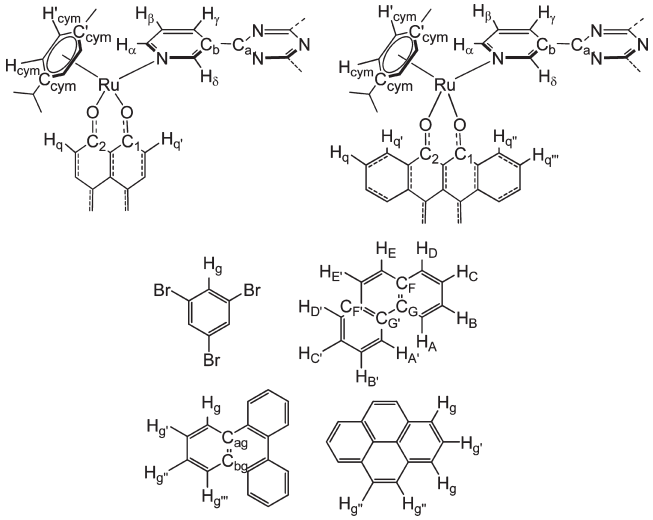

Syntheses of [Template⊂1][CF_3SO_3]$_6$ and [Template⊂2][CF_3SO_3]$_6$. $[Ru_2(p\text{-cymene})_2(OO\cap OO)Cl_2]$ ($OO\cap OO$ = 5,8-dioxido-1,4-naphthoquinonato **1** or 6,11-dioxido-5,12-naphthacenedionato **2**) (**1**, 46.8 mg; **2**, 53.3 mg; 0.064 mmol) and $AgCF_3SO_3$ (33.0 mg, 0.128 mmol) in MeOH (20 mL), 3-tpt (13.4 mg, 0.043 mmol), and an aromatic guest molecule [1,3,5-tribromobenzene (7.2 mg, 0.023 mmol), phenanthrene (4.1 mg, 0.023 mmol), pyrene (4.7 mg, 0.023 mmol), or triphenylene (5.3 mg, 0.023 mmol)] were added. The mixture was stirred at reflux for 24 h and then filtered. The solvent was removed; the dark residue was dissolved in CH_2Cl_2 (3 mL), and diethyl ether was added to precipitate a dark green solid. The solid was filtered and dried under vacuum.

[1,3,5-Tribromobenzene⊂**1**][CF_3SO_3]$_6$: yield 52 mg (65%); UV−vis (1.0×10^{-5} M, CH_2Cl_2) λ_{max} (ε) = 433 nm (4.0×10^4 M^{-1} cm^{-1}), 591 nm (6.4×10^3 M^{-1} cm^{-1}), 640 nm (1.2×10^4 M^{-1} cm^{-1}), 694 nm (1.4×10^4 M^{-1} cm^{-1}); IR (KBr) ν = 3066 cm^{-1} (w, CH_{aryl}), 1534 cm^{-1} (s, C═O), 1275 cm^{-1} (s, CF_3); MS (ESI positive mode) m/z 1599.61 {[**1** + $(CF_3SO_3)_4]^{2+}$}. Anal. Calcd for $C_{138}H_{123}Br_3F_{18}N_{12}O_{30}Ru_6S_6$ (3810.0): C, 43.50; H, 3.25; N, 4.41. Found: C, 43.88; H, 3.51; N, 4.63.

[Phenanthrene⊂**1**][CF_3SO_3]$_6$: yield 60 mg (78%); UV−vis (1.0×10^{-5} M, CH_2Cl_2) λ_{max} (ε) = 431 nm (3.5×10^4 M^{-1} cm^{-1}), 591 nm (7.0×10^3 M^{-1} cm^{-1}), 639 nm (1.1×10^4 M^{-1} cm^{-1}), 694 nm (1.4×10^4 M^{-1} cm^{-1}); IR (KBr) ν = 3066 cm^{-1} (w, CH_{aryl}), 1533 cm^{-1} (s, C═O), 1276 cm^{-1} (s, CF_3); MS (ESI positive mode) m/z 1599.61 {[**1** + $(CF_3SO_3)_4]^{2+}$}. Anal. Calcd for $C_{148}H_{130}F_{18}N_{12}O_{30}Ru_6S_6$ (3673.5): C, 47.74; H, 3.57; N, 4.58. Found: C, 48.01; H, 3.56; N, 4.81.

[Pyrene⊂**1**][CF_3SO_3]$_6$: yield 62 mg (80%); UV−vis (1.0×10^{-5} M, CH_2Cl_2) λ_{max} (ε) = 432 nm (3.4×10^4 M^{-1} cm^{-1}), 591 nm (6.4×10^3 M^{-1} cm^{-1}), 639 nm (1.0×10^4 M^{-1} cm^{-1}), 694 nm (1.3×10^4 M^{-1} cm^{-1}); IR (KBr) ν = 3066 cm^{-1} (w, CH_{aryl}), 1534 cm^{-1} (s, C═O), 1275 cm^{-1} (s, CF_3); MS (ESI positive mode) m/z 1599.61 {[**1** + $(CF_3SO_3)_4]^{2+}$}. Anal. Calcd for $C_{150}H_{130}F_{18}N_{12}O_{30}Ru_6S_6$ (3697.5): C, 48.08; H, 3.54; N, 4.55. Found: C, 48.32; H, 3.38; N, 4.85.

[Triphenylene⊂**1a**][CF_3SO_3]$_6$: yield 70 mg (89%); UV−vis (1.0×10^{-5} M, CH_2Cl_2) λ_{max} (ε) = 435 nm (3.5×10^4 M^{-1} cm^{-1}), 589 nm (6.4×10^3 M^{-1} cm^{-1}), 646 nm (1.0×10^4 M^{-1} cm^{-1}), 699 nm (1.3×10^4 M^{-1} cm^{-1}); IR (KBr) ν = 3065 cm^{-1} (w, CH_{aryl}), 1533 cm^{-1} (s, C═O), 1275 cm^{-1} (s, CF_3); MS (ESI positive mode) m/z 1599.61 {[**1** + $(CF_3SO_3)_4]^{2+}$}. Anal. Calcd for $C_{152}H_{132}F_{18}N_{12}O_{30}Ru_6S_6$ (3723.5): C, 48.39; H, 3.57; N, 4.51. Found: C, 48.57; H, 3.63; N, 4.70.

[1,3,5-Tribromobenzene⊂**2**][CF_3SO_3]$_6$: yield 63 mg (73%); UV−vis (1.0×10^{-5} M, CH_2Cl_2) λ_{max} (ε) = 375 nm (2.6×10^4 M^{-1} cm^{-1}), 527 nm (5.2×10^3 M^{-1} cm^{-1}), 564 nm (1.2×10^4 M^{-1} cm^{-1}), 609 nm (1.8×10^4 M^{-1} cm^{-1}); IR (KBr) ν = 3065 cm^{-1} (w, CH_{aryl}), 1543 cm^{-1} (s, C═O), 1259 cm^{-1} (s, CF_3); MS (ESI positive mode) m/z 1749.20 {[**2** + $(CF_3SO_3)_4]^{2+}$}. Anal. Calcd for $C_{162}H_{135}Br_3F_{18}N_{12}O_{30}Ru_6S_6$ (4110.4): C, 47.34; H, 3.31; N, 4.09. Found: C, 47.45; H, 3.54; N, 4.14.

[Phenanthrene⊂**2**][CF_3SO_3]$_6$: yield 64 mg (77%); UV−vis (1.0×10^{-5} M, CH_2Cl_2) λ_{max} (ε) = 375 nm (2.4×10^4 M^{-1} cm^{-1}), 527 nm (4.9×10^3 M^{-1} cm^{-1}), 565 nm (1.1×10^4 M^{-1} cm^{-1}), 609 nm (1.6×10^4 M^{-1} cm^{-1}); IR (KBr) ν = 3072 cm^{-1} (w, CH_{aryl}), 1544 cm^{-1} (s, C═O), 1260 cm^{-1} (s, CF_3); MS (ESI positive mode) m/z 1749.20 {[**2** + $(CF_3SO_3)_4]^{2+}$}. Anal. Calcd for $C_{170}H_{142}F_{18}N_{12}O_{30}Ru_6S_6$ (3973.8): C, 51.38; H, 3.60; N, 4.23. Found: C, 50.70; H, 3.46; N, 4.27.

[Pyrene⊂**2**][CF_3SO_3]$_6$: yield 72 mg (86%); UV−vis (1.0×10^{-5} M, CH_2Cl_2) λ_{max} (ε) = 375 nm (2.6×10^4 M^{-1} cm^{-1}), 527 nm (5.6×10^3 M^{-1} cm^{-1}), 564 nm (1.2×10^4 M^{-1} cm^{-1}), 608 nm (1.7×10^4 M^{-1} cm^{-1}); IR (KBr) ν = 3072 cm^{-1} (w, CH_{aryl}), 1543 cm^{-1} (s, C═O), 1260 cm^{-1} (s, CF_3); MS (ESI positive mode) m/z 1749.20 {[**2** + $(CF_3SO_3)_4]^{2+}$}. Anal. Calcd for $C_{172}H_{142}F_{18}N_{12}O_{30}Ru_6S_6$ (3997.8): C, 51.67; H, 3.58; N, 4.20. Found: C, 51.55; H, 3.44; N, 3.99.

[Triphenylene⊂**2**][CF_3SO_3]$_6$: yield 67 mg (79%); UV−vis (1.0×10^{-5} M, CH_2Cl_2) λ_{max} (ε) = 377 nm (3.5×10^4 M^{-1} cm^{-1}), 527 nm (6.8×10^3 M^{-1} cm^{-1}), 567 nm (1.5×10^4 M^{-1} cm^{-1}), 610 nm (2.1×10^4 M^{-1} cm^{-1}); IR (KBr) ν = 3074 cm^{-1} (w, CH_{aryl}), 1544 cm^{-1} (s, C═O), 1260 cm^{-1} (s, CF_3); MS (ESI positive mode) m/z 1749.20 {[**2** + $(CF_3SO_3)_4]^{2+}$}, 1863.17 {[**2** + triphenylene + $(CF_3SO_3)_4]^{2+}$}. Anal. Calcd for $C_{174}H_{144}F_{18}N_{12}O_{30}Ru_6S_6$ (4023.9): C, 51.94; H, 3.61; N, 4.18. Found: C, 52.12; H, 3.78; N, 4.38.

NMR Data. [1,3,5-Tribromobenzene⊂**1a**][CF_3SO_3]$_6$: ^1H NMR (400 MHz, CD_3CN) δ 9.47 (s, 6H, H_δ), 8.85 (d, $^3J_{H,H}$ = 8.1 Hz, 6H, H_γ), 8.65 (d, $^3J_{H,H}$ = 5.2 Hz, 6H, H_α), 7.76 (dd, $^3J_{H,H}$ = 5.2 Hz, $^3J_{H,H}$ = 8.1 Hz, 6H, H_β), 7.25 (s, 6H, $H_{q'}$), 7.12 (s, 6H, H_q), 5.74 (d, $^3J_{H,H}$ = 5.9 Hz, 6H, H_{cym}), 5.70 (d, $^3J_{H,H}$ = 5.9 Hz, 6H, H_{cym}), 5.58 (d, $^3J_{H,H}$ = 5.9 Hz, 6H, H'_{cym}), 5.57 (d, $^3J_{H,H}$ = 5.9 Hz, 6H, H'_{cym}), 2.87 [sept, $^3J_{H,H}$ = 7.0 Hz, 6H, $CH(CH_3)_2$], 2.17 (s, 18H, CH_3), 1.37 [d, $^3J_{H,H}$ = 7.0 Hz, 18H, $CH(CH_3)_2$], 1.34 [d, $^3J_{H,H}$ = 7.0 Hz, 18H, $CH(CH_3)_2$]; $^{13}C\{^1H\}$ NMR (100 MHz, CD_3CN) δ 172.0 (C_2), 171.9 (C_1), 169.6 (C_a), 157.0 (CH_α), 153.1 (CH_δ), 139.5 (CH_γ), 138.5 (CH_q, $CH_{q'}$), 133.2 (C_b), 127.5 (CH_β), 112.2 (C_q), 105.1 (C_{cym}), 99.7 (C'_{cym}), 84.8 (CH_{cym}), 84.8 (CH_{cym}), 84.5 (CH'_{cym}), 84.1 (CH'_{cym}), 31.4 [$CH(CH_3)_2$], 22.4 [$CH(CH_3)_2$], 22.2 [$CH(CH_3)_2$], 17.2 (CH_3).

[Phenanthrene⊂**1a**][CF_3SO_3]$_6$: ^1H NMR (400 MHz, CD_3CN) δ 9.05 (s, 6H, H_δ), 8.58 (d, $^3J_{H,H}$ = 5.3 Hz, 6H, H_α), 8.29 (br s, 6H, H_γ), 7.64 (dd, $^3J_{H,H}$ = 5.3 Hz, $^3J_{H,H}$ = 7.7 Hz, 6H, H_β), 7.64 (br s, 6H, $H_{q'}$), 7.40 (s, 6H, H_q), 5.73 (d, $^3J_{H,H}$ = 5.9 Hz, 6H, H_{cym}), 5.63 (d, $^3J_{H,H}$ = 5.9 Hz, 6H, H_{cym}), 5.53 (d, $^3J_{H,H}$ = 5.9

(13) Anderson, H. L.; Anderson, S.; Sanders, J. K. M. *J. Chem. Soc., Perkin Trans. 1* **1995**, 2231–2245.

Hz, 6H, H′$_{cym}$), 5.51 (d, $^3J_{H,H}$ = 5.9 Hz, 6H, H′$_{cym}$), 2.86 [sept, $^3J_{H,H}$ = 6.9 Hz, 6H, C*H*(CH$_3$)$_2$], 2.13 (s, 18H, CH$_3$), 1.34 [d, $^3J_{H,H}$ = 6.9 Hz, 18H, CH(C*H*$_3$)$_2$], 1.29 [d, $^3J_{H,H}$ = 6.9 Hz, 18H, CH(C*H*$_3$)$_2$]; ^{13}C{^{1}H} NMR (100 MHz, CD$_3$CN) δ 172.2 (*C*$_2$), 171.6 (*C*$_1$), 168.2 (*C*$_a$), 156.4 (*C*H$_\alpha$), 152.3 (*C*H$_\delta$), 139.3 (*C*H$_{q'}$), 139.2 (*C*H$_\gamma$), 138.7 (*C*H$_q$), 132.7 (*C*$_b$), 127.2 (*C*H$_\beta$), 112.4 (*C*$_q$), 105.0 (*C*$_{cym}$), 99.8 (*C*′$_{cym}$), 85.0 (*C*H$_{cym}$), 84.7 (*C*H$_{cym}$), 84.4 (*C*H′$_{cym}$), 84.3 (*C*H′$_{cym}$), 31.3 [*C*H(CH$_3$)$_2$], 22.3 [CH(*C*H$_3$)$_2$], 22.1 [CH(*C*H$_3$)$_2$], 17.2 (*C*H$_3$).

[Pyrene⊂**1a**][CF$_3$SO$_3$]$_6$: ^{1}H NMR (400 MHz, CD$_3$CN) δ 9.45 (br s, 6H, H$_\delta$), 8.84 (br s, 6H, H$_\gamma$), 8.61 (br s, 6H, H$_\alpha$), 7.71 (br s, 6H, H$_\beta$), 7.45 (br s, 6H, H$_{q'}$), 7.28 (br s, 6H, H$_q$), 5.52 (br s, 24H, H$_{cym}$), 2.86 [br s, 6H, C*H*(CH$_3$)$_2$], 2.10 (br s, 18H, CH$_3$), 1.30 [br s, 36H, CH(C*H*$_3$)$_2$]. Because of the broadness of the signals, it was not possible to record the ^{13}C NMR data.

[Template⊂**1b**][CF$_3$SO$_3$]$_6$: ^{1}H NMR (400 MHz, CD$_3$CN) δ 9.03 (s, 6H, H$_\delta$), 8.42 (d, $^3J_{H,H}$ = 5.3 Hz, 6H, H$_\alpha$), 7.81 (d, $^3J_{H,H}$ = 8.0 Hz, 6H, H$_\gamma$), 7.76 (br s, 6H, H$_{q'}$), 7.50 (br s, 6H, H$_q$), 7.12 (dd, $^3J_{H,H}$ = 5.3 Hz, $^3J_{H,H}$ = 8.0 Hz, 6H, H$_\beta$), 5.72 (d, $^3J_{H,H}$ = 5.9 Hz, 6H, H$_{cym}$), 5.65 (d, $^3J_{H,H}$ = 5.9 Hz, 6H, H$_{cym}$), 5.53 (d, $^3J_{H,H}$ = 5.9 Hz, 6H, H′$_{cym}$), 5.50 (d, $^3J_{H,H}$ = 5.9 Hz, 6H, H′$_{cym}$), 2.86 [sept, $^3J_{H,H}$ = 6.9 Hz, 6H, C*H*(CH$_3$)$_2$], 2.10 (s, 18H, CH$_3$), 1.32 [d, $^3J_{H,H}$ = 6.9 Hz, 18H, CH(C*H*$_3$)$_2$], 1.29 [d, $^3J_{H,H}$ = 6.9 Hz, 18H, CH(C*H*$_3$)$_2$]; ^{13}C{^{1}H} NMR (100 MHz, CD$_3$CN) δ 172.0 (*C*$_2$), 171.9 (*C*$_1$), 169.2 (*C*$_a$), 156.8 (*C*H$_\alpha$), 152.0 (*C*H$_\delta$), 138.9 (*C*H$_{q'}$, *C*H$_q$), 138.0 (*C*H$_\gamma$), 132.2 (*C*$_b$), 126.9 (*C*H$_\beta$), 112.2 (*C*$_q$), 105.1 (*C*$_{cym}$), 99.8 (*C*′$_{cym}$), 85.0 (*C*H$_{cym}$), 84.8 (*C*H$_{cym}$), 84.5 (*C*H′$_{cym}$), 84.3 (*C*H′$_{cym}$), 31.4 [*C*H(CH$_3$)$_2$], 22.4 [CH(*C*H$_3$)$_2$], 22.1 [CH(*C*H$_3$)$_2$], 17.2 (*C*H$_3$).

[Triphenylene⊂**1a**][CF$_3$SO$_3$]$_6$: ^{1}H NMR (400 MHz, CD$_3$CN) δ 8.83 (s, 6H, H$_\delta$), 8.51 (d, $^3J_{H,H}$ = 5.2 Hz, 6H, H$_\alpha$), 7.95 (d, $^3J_{H,H}$ = 8.0 Hz, 6H, H$_\gamma$), 7.89 (s, 6H, H$_{q'}$), 7.53 (dd, $^3J_{H,H}$ = 5.2 Hz, $^3J_{H,H}$ = 8.0 Hz, 6H, H$_\beta$), 7.49 (s, 6H, H$_q$), 7.35 (d, $^3J_{H,H}$ = 8.1 Hz, 3H, H$_g$), 6.49 (t, $^3J_{H,H}$ = 8.1 Hz, 3H, H$_{g'}$), 5.79 (d, $^3J_{H,H}$ = 8.1 Hz, 3H, H$_{g'''}$), 5.72 (d, $^3J_{H,H}$ = 5.9 Hz, 6H, H$_{cym}$), 5.58 (d, $^3J_{H,H}$ = 5.9 Hz, 6H, H$_{cym}$), 5.51 (d, $^3J_{H,H}$ = 5.9 Hz, 6H, H′$_{cym}$), 5.46 (d, $^3J_{H,H}$ = 5.9 Hz, 6H, H′$_{cym}$), 4.02 (t, $^3J_{H,H}$ = 8.1 Hz, 3H, H$_{g''}$), 2.85 [sept, $^3J_{H,H}$ = 6.9 Hz, 6H, C*H*(CH$_3$)$_2$], 2.10 (s, 18H, CH$_3$), 1.32 [d, $^3J_{H,H}$ = 6.9 Hz, 18H, CH(C*H*$_3$)$_2$], 1.27 [d, $^3J_{H,H}$ = 6.9 Hz, 18H, CH(C*H*$_3$)$_2$]; ^{13}C{^{1}H} NMR (100 MHz, CD$_3$CN) δ 172.3 (*C*$_2$), 171.3 (*C*$_1$), 167.7 (*C*$_a$), 156.2 (*C*H$_\alpha$), 151.8 (*C*H$_\delta$), 139.7 (*C*H$_{q'}$), 139.2 (*C*H$_\gamma$), 138.7 (*C*H$_q$), 132.1 (*C*$_b$), 129.3 (*C*H$_{g'}$), 128.8 (*C*$_{ag}$), 127.9 (*C*$_{bg}$), 126.7 (*C*H$_\beta$), 124.9 (*C*H$_{g''}$), 123.0 (*C*H$_g$), 122.3 (*C*H$_{g'''}$), 112.5 (*C*$_q$), 104.9 (*C*$_{cym}$), 99.9 (*C*′$_{cym}$), 85.2 (*C*H$_{cym}$), 84.6 (*C*H$_{cym}$), 84.4 (*C*H′$_{cym}$), 84.3 (*C*H′$_{cym}$), 31.3 [*C*H(CH$_3$)$_2$], 22.3 [CH(*C*H$_3$)$_2$], 22.0 [CH(*C*H$_3$)$_2$], 17.1 (*C*H$_3$).

[1,3,5-Tribromobenzene⊂**2**][CF$_3$SO$_3$]$_6$: ^{1}H NMR (400 MHz, CD$_3$CN) δ 9.45 (d, $^4J_{H,H}$ = 1.3 Hz, 6H, H$_\delta$), 8.88 (dd, $^3J_{H,H}$ = 3.4 Hz, $^3J_{H,H}$ = 6.1 Hz, 6H, H$_{q'}$), 8.84 (dd, $^3J_{H,H}$ = 3.4 Hz, $^3J_{H,H}$ = 6.1 Hz, 6H, H$_{q''}$), 8.82 (d, $^3J_{H,H}$ = 7.9 Hz, 6H, H$_\gamma$), 8.79 (d, $^3J_{H,H}$ = 5.7 Hz, 6H, H$_q$), 8.06 (dd, $^3J_{H,H}$ = 3.4 Hz, $^3J_{H,H}$ = 6.1 Hz, 6H, H$_q$), 7.90 (dd, $^3J_{H,H}$ = 5.7 Hz, $^3J_{H,H}$ = 7.9 Hz, 6H, H$_\beta$), 7.47 (dd, $^3J_{H,H}$ = 3.4 Hz, $^3J_{H,H}$ = 6.1 Hz, 6H, H$_{q'''}$), 5.94 (d, $^3J_{H,H}$ = 6.2 Hz, 6H, H$_{cym}$), 5.91 (d, $^3J_{H,H}$ = 6.2 Hz, 6H, H$_{cym}$), 5.75 (d, $^3J_{H,H}$ = 6.2 Hz, 6H, H′$_{cym}$), 5.74 (d, $^3J_{H,H}$ = 6.2 Hz, 6H, H′$_{cym}$), 3.52 (s, 3H, H$_g$), 2.96 [sept, $^3J_{H,H}$ = 6.9 Hz, 6H, C*H*(CH$_3$)$_2$], 2.15 (s, 18H, CH$_3$), 1.32 [d, $^3J_{H,H}$ = 6.9 Hz, 18H, CH(C*H*$_3$)$_2$], 1.30 [d, $^3J_{H,H}$ = 6.9 Hz, 18H, CH(C*H*$_3$)$_2$]; ^{13}C{^{1}H} NMR (100 MHz, CD$_3$CN) δ 170.4 (*C*$_2$), 169.7 (*C*$_1$), 169.0 (*C*$_a$), 157.1 (*C*H$_\alpha$), 152.9 (*C*H$_\delta$), 139.3 (*C*H$_\gamma$), 135.0 (*C*$_q$), 134.8 (*C*$_q$), 134.2 (*C*H$_q$), 133.9 (*C*H$_{q'''}$), 133.0 (*C*$_b$), 131.1 (*C*H$_g$), 128.4 (*C*H$_{q'}$), 127.6 (*C*H$_{q''}$), 127.4 (*C*H$_\beta$), 121.5 (*C*$_g$), 107.8 (*C*$_q$), 105.0 (*C*$_{cym}$), 100.4 (*C*′$_{cym}$), 85.0 (*C*H$_{cym}$), 84.5 (*C*H$_{cym}$), 83.9 (*C*H′$_{cym}$), 83.6 (*C*H′$_{cym}$), 31.4 [*C*H(CH$_3$)$_2$], 22.6 [CH(*C*H$_3$)$_2$], 22.3 [CH(*C*H$_3$)$_2$], 17.9 (*C*H$_3$).

[Phenanthrene⊂**2**][CF$_3$SO$_3$]$_6$: ^{1}H NMR (400 MHz, CD$_3$CN) δ 9.02 (dd, $^3J_{H,H}$ = 3.4 Hz, $^3J_{H,H}$ = 6.1 Hz, 6H, H$_{q''}$), 8.96 (dd, $^3J_{H,H}$ = 3.4 Hz, $^3J_{H,H}$ = 6.1 Hz, 6H, H$_{q'}$), 8.92 (s, 6H, H$_\delta$), 8.65 (d, $^3J_{H,H}$ = 5.7 Hz, 6H, H$_\alpha$), 8.14 (dd, $^3J_{H,H}$ = 3.4 Hz, $^3J_{H,H}$ = 6.1 Hz, 6H, H$_q$), 8.06 (dd, $^3J_{H,H}$ = 3.4 Hz, $^3J_{H,H}$ = 6.1 Hz, 6H, H$_{q'''}$), 7.94 (d, $^3J_{H,H}$ = 7.7 Hz, 6H, H$_\gamma$), 7.59 (dd, $^3J_{H,H}$ = 5.7 Hz, $^3J_{H,H}$ = 7.7 Hz, 6H, H$_\beta$), 5.92 (d, $^3J_{H,H}$ = 6.0 Hz, 6H, H$_{cym}$), 5.80 (d, $^3J_{H,H}$ = 6.0 Hz, 6H, H$_{cym}$), 5.67 (d, $^3J_{H,H}$ = 6.0 Hz, 6H, H′$_{cym}$), 5.62 (d, $^3J_{H,H}$ = 6.0 Hz, 6H, H′$_{cym}$), 5.45 (t, $^3J_{H,H}$ = 7.7 Hz, 1H, H$_C$), 5.09 (d, $^3J_{H,H}$ = 7.7 Hz, 1H, H$_A$), 4.99 (t, $^3J_{H,H}$ = 7.7 Hz, 1H, H$_{B'}$), 4.86 (d, $^3J_{H,H}$ = 7.7 Hz, 1H, H$_{A'}$), 4.42 (q, $^3J_{H,H}$ = 8.7 Hz, 2H, H$_{E,E'}$), 4.29 (d, $^3J_{H,H}$ = 7.7 Hz, 1H, H$_D$), 4.08 (d, $^3J_{H,H}$ = 7.7 Hz, 1H, H$_{D'}$), 3.70 (m, 2H, H$_{B,C'}$), 2.94 [sept, $^3J_{H,H}$ = 6.8 Hz, 6H, C*H*(CH$_3$)$_2$], 2.11 (s, 18H, CH$_3$), 1.30 [d, $^3J_{H,H}$ = 6.8 Hz, 18H, CH(C*H*$_3$)$_2$], 1.25 [d, $^3J_{H,H}$ = 6.8 Hz, 18H, CH(C*H*$_3$)$_2$]; ^{13}C{^{1}H} NMR (100 MHz, CD$_3$CN) δ 170.5 (*C*$_2$), 169.2 (*C*$_1$), 167.5 (*C*$_a$), 156.1 (*C*H$_\alpha$), 151.9 (*C*H$_\delta$), 138.9 (*C*H$_\gamma$), 135.2 (*C*$_q$), 134.8 (*C*$_q$), 134.4 (*C*H$_q$), 134.3 (*C*H$_{q'''}$), 132.4 (*C*$_b$), 131.2 (*C*$_F$), 129.8 (*C*$_{F'}$), 128.6 (*C*H$_{q''}$), 128.5 (*C*H$_{q'}$), 128.4 (*C*H$_{B'}$), 128.1 (*C*H$_C$), 128.0 (*C*$_{G'}$), 127.3 (*C*$_G$), 127.3 (*C*H$_{D'}$), 127.0 (*C*H$_D$), 127.0 (*C*H$_{E'}$), 126.8 (*C*H$_\beta$), 126.4 (*C*H$_E$), 124.2 (*C*H$_{C'}$), 123.6 (*C*H$_B$), 120.3 (*C*H$_A$), 120.1 (*C*H$_{A'}$), 108.1 (*C*$_q$), 104.7 (*C*$_{cym}$), 100.5 (*C*′$_{cym}$), 85.3 (*C*H$_{cym}$), 84.7 (*C*H$_{cym}$), 83.6 (*C*H′$_{cym}$), 83.4 (*C*H′$_{cym}$), 31.4 [*C*H(CH$_3$)$_2$], 22.5 [CH(*C*H$_3$)$_2$], 22.2 [CH(*C*H$_3$)$_2$], 17.8 (*C*H$_3$).

[Pyrene⊂**2**][CF$_3$SO$_3$]$_6$: ^{1}H NMR (400 MHz, CD$_3$CN) δ 9.05 (dd, $^3J_{H,H}$ = 3.4 Hz, $^3J_{H,H}$ = 6.0 Hz, 6H, H$_{q''}$), 8.99 (dd, $^3J_{H,H}$ = 3.4 Hz, $^3J_{H,H}$ = 6.0 Hz, 6H, H$_{q'}$), 8.65 (dd, $^3J_{H,H}$ = 5.7 Hz, $^4J_{H,H}$ = 1.0 Hz, 6H, H$_\alpha$), 8.64 (d, $^4J_{H,H}$ = 1.4 Hz, 6H, H$_\delta$), 8.22 (dd, $^3J_{H,H}$ = 3.4 Hz, $^3J_{H,H}$ = 6.0 Hz, 6H, H$_{q'''}$), 8.16 (dd, $^3J_{H,H}$ = 3.4 Hz, $^3J_{H,H}$ = 6.0 Hz, 6H, H$_q$), 7.71 (dd, $^3J_{H,H}$ = 8.0 Hz, $^4J_{H,H}$ = 1.4 Hz, 6H, H$_\gamma$), 7.54 (dd, $^3J_{H,H}$ = 5.7 Hz, $^3J_{H,H}$ = 8.0 Hz, 6H, H$_\beta$), 5.94 (d, $^3J_{H,H}$ = 5.9 Hz, 6H, H$_{cym}$), 5.76 (d, $^3J_{H,H}$ = 5.9 Hz, 6H, H$_{cym}$), 5.64 (d, $^3J_{H,H}$ = 5.9 Hz, 6H, H′$_{cym}$), 5.57 (d, $^3J_{H,H}$ = 5.9 Hz, 6H, H′$_{cym}$), 5.10 (d, $^3J_{H,H}$ = 7.5 Hz, 2H, H$_g$), 4.77 (d, $^3J_{H,H}$ = 7.5 Hz, 2H, H$_{g'}$), 4.65 (d, $^3J_{H,H}$ = 8.9 Hz, 2H, H$_{g''}$), 4.58 (t, $^3J_{H,H}$ = 7.5 Hz, 2H, H$_{g'''}$), 4.43 (d, $^3J_{H,H}$ = 8.9 Hz, 2H, H$_{g''''}$), 2.95 [sept, $^3J_{H,H}$ = 6.9 Hz, 6H, C*H*(CH$_3$)$_2$], 2.09 (s, 18H, CH$_3$), 1.29 [d, $^3J_{H,H}$ = 6.9 Hz, 18H, CH(C*H*$_3$)$_2$], 1.25 [d, $^3J_{H,H}$ = 6.9 Hz, 18H, CH(C*H*$_3$)$_2$]; ^{13}C{^{1}H} NMR (100 MHz, CD$_3$CN) δ 170.5 (*C*$_2$), 169.3 (*C*$_1$), 166.4 (*C*$_a$), 156.1 (*C*H$_\alpha$), 151.7 (*C*H$_\delta$), 138.9 (*C*H$_\gamma$), 135.8 (*C*$_q$), 134.9 (*C*$_q$), 134.4 (*C*H$_{q'''}$), 134.3 (*C*H$_q$), 132.2 (*C*$_b$), 129.1 (*C*$_g$), 128.8 (*C*H$_{q''}$), 128.4 (*C*H$_{q'}$), 126.7 (*C*H$_{g''}$), 126.7 (*C*H$_\beta$), 125.7 (*C*H$_{g''''}$), 124.8 (*C*H$_{g'}$), 124.7 (*C*H$_g$), 124.4 (*C*H$_{g'''}$), 121.5 (*C*$_g$), 108.1 (*C*$_q$), 104.5 (*C*$_{cym}$), 100.6 (*C*′$_{cym}$), 85.5 (*C*H$_{cym}$), 84.8 (*C*H$_{cym}$), 83.4 (*C*H′$_{cym}$), 83.3 (*C*H′$_{cym}$), 31.4 [*C*H(CH$_3$)$_2$], 22.5 [CH(*C*H$_3$)$_2$], 22.2 [CH(*C*H$_3$)$_2$], 17.7 (*C*H$_3$).

[Triphenylene⊂**2**][CF$_3$SO$_3$]$_6$: ^{1}H NMR (400 MHz, CD$_3$CN) δ 9.08 (dd, $^3J_{H,H}$ = 3.4 Hz, $^3J_{H,H}$ = 6.1 Hz, 6H, H$_{q''}$), 8.97 (dd, $^3J_{H,H}$ = 3.4 Hz, $^3J_{H,H}$ = 6.1 Hz, 6H, H$_{q'}$), 8.81 (d, $^4J_{H,H}$ = 1.6 Hz, 6H, H$_\delta$), 8.58 (dd, $^3J_{H,H}$ = 5.5 Hz, $^4J_{H,H}$ = 1.0 Hz, 6H, H$_\alpha$), 8.24 (dd, $^3J_{H,H}$ = 3.4 Hz, $^3J_{H,H}$ = 6.1 Hz, 6H, H$_{q'''}$), 8.17 (dd, $^3J_{H,H}$ = 3.4 Hz, $^3J_{H,H}$ = 6.1 Hz, 6H, H$_q$), 7.73 (dd, $^3J_{H,H}$ = 7.9 Hz, $^4J_{H,H}$ = 1.6 Hz, 6H, H$_\gamma$), 7.49 (dd, $^3J_{H,H}$ = 5.5 Hz, $^3J_{H,H}$ = 7.9 Hz, 6H, H$_\beta$), 5.93 (d, $^3J_{H,H}$ = 5.9 Hz, 6H, H$_{cym}$), 5.79 (d, $^3J_{H,H}$ = 5.9 Hz, 6H, H$_{cym}$), 5.65 (d, $^3J_{H,H}$ = 5.9 Hz, 6H, H′$_{cym}$), 5.61 (d, $^3J_{H,H}$ = 5.9 Hz, 6H, H′$_{cym}$), 5.39 (t, $^3J_{H,H}$ = 7.9 Hz, 3H, H$_{g'}$), 5.29 (d, $^3J_{H,H}$ = 7.9 Hz, 3H, H$_{g'''}$), 5.00 (d, $^3J_{H,H}$ = 7.9 Hz, 3H, H$_g$), 3.72 (t, $^3J_{H,H}$ = 7.9 Hz, 3H, H$_{g''}$), 2.93 [sept, $^3J_{H,H}$ = 6.9 Hz, 6H, C*H*(CH$_3$)$_2$], 2.09 (s, 18H, CH$_3$), 1.29 [d, $^3J_{H,H}$ = 6.9 Hz, 18H, CH(C*H*$_3$)$_2$], 1.24 [d, $^3J_{H,H}$ = 6.9 Hz, 18H, CH(C*H*$_3$)$_2$]; ^{13}C{^{1}H} NMR (100 MHz, CD$_3$CN) δ 170.4 (*C*$_2$), 169.1 (*C*$_1$), 167.4 (*C*$_a$), 155.8 (*C*H$_\alpha$), 151.7 (*C*H$_\delta$), 139.0 (*C*H$_\gamma$), 135.2 (*C*$_q$), 134.6 (*C*H$_{q'''}$), 134.5 (*C*H$_q$), 131.7 (*C*$_b$), 129.4 (*C*H$_{g'}$), 128.7 (*C*H$_{q''}$), 128.5 (*C*H$_{q'}$), 128.3 (*C*$_{ag}$), 127.3 (*C*$_{bg}$), 126.4 (*C*H$_\beta$), 124.3 (*C*H$_{g''}$), 121.6 (*C*H$_{g'''}$), 121.0 (*C*H$_g$), 108.0 (*C*$_q$), 104.7 (*C*$_{cym}$), 100.5 (*C*′$_{cym}$), 85.3 (*C*H$_{cym}$), 84.7 (*C*H$_{cym}$), 83.5 (*C*H′$_{cym}$), 83.4 (*C*H′$_{cym}$), 31.3 [*C*H(CH$_3$)$_2$], 22.5 [CH(*C*H$_3$)$_2$], 22.2 [CH(*C*H$_3$)$_2$], 17.8 (*C*H$_3$).

Isolation of Empty Cages [1][CF$_3$SO$_3$]$_6$ and [2][CF$_3$SO$_3$]$_6$. [1,3,5-Tribromobenzene⊂**1**][CF$_3$SO$_3$]$_6$ (90 mg, 0.024 mmol) or [1,3,5-tribromobenzene⊂**2**][CF$_3$SO$_3$]$_6$ (90 mg, 0.022 mmol) in toluene (200 mL) was stirred at reflux for 12 h and then filtered. This step was repeated three times, and the final dark green solid

was filtered, washed with diethyl ether, and dried under vacuum to afford empty complexes [**1**][CF_3SO_3]$_6$ and [**2**][CF_3SO_3]$_6$.

[**1**][CF_3SO_3]$_6$: yield 70 mg (85%); UV−vis (1.0×10^{-5} M, CH_2Cl_2) λ_{max} (ε) = 433 nm (3.6×10^4 M^{-1} cm^{-1}), 591 nm (6.5×10^3 M^{-1} cm^{-1}), 639 nm (1.2×10^4 M^{-1} cm^{-1}), 694 nm (1.4×10^4 M^{-1} cm^{-1}); IR (KBr) ν = 3066 cm^{-1} (w, CH_{aryl}), 1533 cm^{-1} (s, C═O), 1275 cm^{-1} (s, CF_3); ^{1}H NMR (400 MHz, CD_3CN) δ 9.42 (s, 6H, H_δ), 9.03 (s, 6H, H_δ), 8.79 (br s, 6H, H_γ), 8.65 (d, $^3J_{H,H}$ = 5.2 Hz, 6H, H_α), 8.42 (br s, 6H, H_α), 7.81 (d, $^3J_{H,H}$ = 7.8 Hz, 6H, H_γ), 7.76 (br s, 6H, $H_{q'}$), 7.76 (br s, 6H, H_β), 7.50 (br s, 6H, H_q), 7.27 (s, 6H, $H_{q'}$), 7.19 (s, 6H, H_q), 7.09 (br s, 6H, H_β), 5.74 (d, $^3J_{H,H}$ = 5.9 Hz, 6H, H_{cym}), 5.72 (d, $^3J_{H,H}$ = 5.9 Hz, 6H, H_{cym}), 5.69 (d, $^3J_{H,H}$ = 5.9 Hz, 6H, H_{cym}), 5.65 (d, $^3J_{H,H}$ = 5.9 Hz, 6H, H_{cym}), 5.58 (d, $^3J_{H,H}$ = 5.9 Hz, 6H, H'_{cym}), 5.56 (d, $^3J_{H,H}$ = 5.9 Hz, 6H, H'_{cym}), 5.53 (d, $^3J_{H,H}$ = 5.9 Hz, 6H, H'_{cym}), 5.51 (d, $^3J_{H,H}$ = 5.9 Hz, 6H, H'_{cym}), 2.87 [sept, $^3J_{H,H}$ = 6.9 Hz, 12H, $CH(CH_3)_2$], 2.17 (s, 18H, CH_3), 2.10 (s, 18H, CH_3), 1.37 [d, $^3J_{H,H}$ = 7.0 Hz, 18H, $CH(CH_3)_2$], 1.33 [d, $^3J_{H,H}$ = 7.0 Hz, 18H, $CH(CH_3)_2$], 1.32 [d, $^3J_{H,H}$ = 6.9 Hz, 18H, $CH(CH_3)_2$], 1.29 [d, $^3J_{H,H}$ = 6.9 Hz, 18H, $CH(CH_3)_2$]; $^{13}C\{^1H\}$ NMR (100 MHz, CD_3CN) δ 172.0 (C_2), 171.9 (C_1), 169.6 (C_a), 169.2 (C_a), 157.0 (CH_α), 156.8 (CH_α), 153.1 (CH_δ), 152.0 (CH_δ), 139.5 (CH_γ), 138.9 (CH_q, $CH_{q'}$), 138.5 (CH_q, $CH_{q'}$), 138.0 (CH_γ), 133.2 (C_b), 132.2 (C_b), 127.5 (CH_β), 126.9 (CH_β), 112.2 (C_q), 105.1 (C_{cym}), 99.8 (C'_{cym}), 99.7 (C'_{cym}), 85.0 (CH_{cym}), 84.8 (CH_{cym}, CH_{cym}, CH_{cym}), 84.5 (CH'_{cym}, CH'_{cym}), 84.3 (CH'_{cym}), 84.1 (CH'_{cym}), 31.4 [$CH(CH_3)_2$, $CH'(CH_3)_2$], 22.4 [$CH(CH_3)_2$], 22.4 [$CH(CH_3)_2$], 22.2 [$CH(CH_3)_2$], 22.1 [$CH(CH_3)_2$], 17.2 (CH_3), 17.2 (CH_3); MS (ESI positive mode) m/z 1599.61 {[**1** + $(CF_3SO_3)_4]^{2+}$}. Anal. Calcd for $C_{132}H_{120}F_{18}N_{12}O_{30}Ru_6S_6$ (3495.2): C, 45.36; H, 3.46; N, 4.81. Found: C, 45.56; H, 3.55; N, 4.92.

[**2**][CF_3SO_3]$_6$: yield 72 mg (87%); UV−vis (1.0×10^{-5} M, CH_2Cl_2) λ_{max} (ε) = 375 nm (2.2×10^4 M^{-1} cm^{-1}), 527 nm (4.8×10^3 M^{-1} cm^{-1}), 564 nm (1.1×10^4 M^{-1} cm^{-1}), 609 nm (1.5×10^4 M^{-1} cm^{-1}); IR (KBr) ν = 3066 cm^{-1} (w, CH_{aryl}), 1543 cm^{-1} (s, C═O), 1260 cm^{-1} (s, CF_3); ^{1}H NMR (400 MHz, CD_3CN) δ 9.51 (s, 6H, H_δ), 8.86 (dd, $^3J_{H,H}$ = 3.4 Hz, $^3J_{H,H}$ = 6.1 Hz, 6H, $H_{q'}$), 8.81 (d, $^3J_{H,H}$ = 5.7 Hz, 6H, H_q), 8.80 (d, $^3J_{H,H}$ = 8.0 Hz, 6H, H_γ), 8.74 (dd, $^3J_{H,H}$ = 3.4 Hz, $^3J_{H,H}$ = 6.1 Hz, 6H, $H_{q''}$), 8.05 (dd, $^3J_{H,H}$ = 3.4 Hz, $^3J_{H,H}$ = 6.1 Hz, 6H, H_q), 7.87 (dd, $^3J_{H,H}$ = 5.7 Hz, $^3J_{H,H}$ = 8.0 Hz, 6H, H_β), 7.44 (dd, $^3J_{H,H}$ = 3.4 Hz, $^3J_{H,H}$ = 6.1 Hz, 6H, $H_{q'''}$), 5.94 (d, $^3J_{H,H}$ = 5.7 Hz, 6H, H_{cym}), 5.91 (d, $^3J_{H,H}$ = 5.7 Hz, 6H, H_{cym}), 5.76 (d, $^3J_{H,H}$ = 5.7 Hz, 6H, H'_{cym}), 5.75 (d, $^3J_{H,H}$ = 5.7 Hz, 6H, H'_{cym}), 2.97 [sept, $^3J_{H,H}$ = 6.9 Hz, 6H, $CH(CH_3)_2$], 2.14 (s, 18H, CH_3), 1.32 [d, $^3J_{H,H}$ = 6.9 Hz, 18H, $CH(CH_3)_2$], 1.31 [d, $^3J_{H,H}$ = 6.9 Hz, 18H, $CH(CH_3)_2$]; $^{13}C\{^1H\}$ NMR (100 MHz, CD_3CN) δ 170.5 (C_2), 169.3 (C_1), 169.2 (C_a), 157.3 (CH_α), 152.7 (CH_δ), 139.3 (CH_γ), 134.8 (C_q), 134.6 (C_q), 134.2 (CH_q), 133.4 ($CH_{q'''}$), 133.0 (C_b), 128.4 ($CH_{q'}$), 127.7 ($CH_{q''}$), 127.6 (CH_β), 107.8 (C_q), 105.0 (C_{cym}), 100.4 (C'_{cym}), 85.0 (CH_{cym}), 84.4 (CH_{cym}), 83.9 (CH'_{cym}), 83.7 (CH'_{cym}), 31.4 [$CH(CH_3)_2$], 22.6 [$CH(CH_3)_2$], 22.2 [$CH(CH_3)_2$], 17.9 (CH_3); MS (ESI positive mode) m/z 1749.20 {[**2** + $(CF_3SO_3)_4]^{2+}$}. Anal. Calcd for $C_{156}H_{132}F_{18}N_{12}O_{30}Ru_6S_6$ (3795.6): C, 49.37; H, 3.51; N, 4.43. Found: C, 49.22; H, 3.34; N, 4.35.

NMR Experiments. DOSY NMR Experiments. For all DOSY experiments, the temperature was regulated at 298 K, the rate of air flow was increased to 670 L/min, and the NMR tube was spun. The diffusion NMR experiments were performed using a standard pulse-gradient stimulated echo (LED-PFGSTE) sequence, using a bipolar gradient.[8a,b] DOSY spectra were generated by using TopSpin version 2.0 (Bruker). Experimental parameters were as follows: Δ = 50 ms (diffusion delay), τ = 1.0 ms (gradient recovery delay), and Te = 5 ms (eddy current recovery delay). For each data set, 4096 complex points were collected, and the gradient dimension was sampled using 32 experiments in which the gradient strength was exponentially incremented from 1 to 50.8 G/cm. The gradient duration $\delta/2$ was adjusted to observe a nearly complete signal loss at 50.8 G/cm. Typically, the $\delta/2$ delay was set in the 1.8−2.0 ms range. A 1 s recycle delay was used between scans for data shown. For each data set, the spectral axis was processed with an exponential function (3−5 Hz line broadening), and a Fourier transform was applied to obtain 4096 real points. The DOSY reconstruction was realized with 256 points in the diffusion dimension. The number of scans ranged from 16 to 64 and was adapted to each sample, while the experimental time ranged from 8 to 60 min.

ROESY NMR Experiments. The 1D ROESY NMR experiments were performed using a gradient-selected ROESY experiment.[14] Experimental parameters were as follows: τ_m = 200 ms (mixing time), δ = 500 μs (gradient length), G_0 = 1 G/cm, G_1 = 3 G/cm, G_2 = 6 G/cm (gradient strength), and τ_p = 100 ms (selective pulse, Seduce-1); 8192 complex points were collected. A 3 s recycle delay was used. The spectral axis was processed with an exponential function (3 Hz line broadening), and a Fourier transform was applied to obtain 8192 real points.

EXSY NMR Experiments. The 1D EXSY NMR experiments were performed using a gradient-selected NOESY/EXSY experiment.[11] The plots of the diagonal and cross-peak as a function of mixing time τ_m have been obtained using 12 τ_m values ranging from 1 ms to 2 s. Other experimental parameters are identical to those used for the original version;[11] 4096 complex points were collected, leading to an acquisition time of 0.51 s. The T_1 relaxation times of the target diagonal and the cross-peaks were obtained using a classical inversion recovery experiment and ranged from 1.3 to 1.6 s. To ensure quantitative conditions, a 8 s recycle delay was used. The spectral axis was processed with an exponential function (3 Hz line broadening), and a Fourier transform was applied to obtain 8192 real points. The number of scans ranged from 16 to 64 and was adapted to each sample.

Acknowledgment. Financial support of this work by the Swiss National Science Foundation and a generous loan of ruthenium(III) chloride hydrate by the Johnson Matthey Research Centre are gratefully acknowledged.

Supporting Information Available: ESI-MS spectra of [**1**][CF_3SO_3]$_6$ and [**2**][CF_3SO_3]$_6$ and selected ^{1}H, COSY, DOSY, variable-temperature measurement, 1D EXSY, and ROESY spectra of the different [**cage**]$^{6+}$ and [template⊂**cage**]$^{6+}$ systems. This material is available free of charge via the Internet at http://pubs.acs.org.

(14) Furrer, J. *J. Nat. Prod.* **2009**, *72*, 1437–1441.